Published in "Development doi: 10.1242/dev.113225, 2015"
which should be cited to refer to this work.

The cyclophilin A DIAGEOTROPICA gene affects auxin transport in both root and shoot to control lateral root formation

Maria G. Ivanchenko[1,*], Jinsheng Zhu[2], Bangjun Wang[2,8], Eva Medvecká[3], Yunlong Du[4,5], Elisa Azzarello[6], Stefano Mancuso[6], Molly Megraw[1], Sergei Filichkin[1], Joseph G. Dubrovsky[7], Jiří Friml[3,4] and Markus Geisler[2]

ABSTRACT

Cyclophilin A is a conserved peptidyl-prolyl *cis-trans* isomerase (PPIase) best known as the cellular receptor of the immunosuppressant cyclosporine A. Despite significant effort, evidence of developmental functions of cyclophilin A in non-plant systems has remained obscure. Mutations in a tomato (*Solanum lycopersicum*) cyclophilin A ortholog, DIAGEOTROPICA (DGT), have been shown to abolish the organogenesis of lateral roots; however, a mechanistic explanation of the phenotype is lacking. Here, we show that the *dgt* mutant lacks auxin maxima relevant to priming and specification of lateral root founder cells. DGT is expressed in shoot and root, and localizes to both the nucleus and cytoplasm during lateral root organogenesis. Mutation of ENTIRE/IAA9, a member of the auxin-responsive Aux/IAA protein family of transcriptional repressors, partially restores the inability of *dgt* to initiate lateral root primordia but not the primordia outgrowth. By comparison, grafting of a wild-type scion restores the process of lateral root formation, consistent with participation of a mobile signal. Antibodies do not detect movement of the DGT protein into the *dgt* rootstock; however, experiments with radiolabeled auxin and an auxin-specific microelectrode demonstrate abnormal auxin fluxes. Functional studies of DGT in heterologous yeast and tobacco-leaf auxin-transport systems demonstrate that DGT negatively regulates PIN-FORMED (PIN) auxin efflux transporters by affecting their plasma membrane localization. Studies in tomato support complex effects of the *dgt* mutation on PIN expression level, expression domain and plasma membrane localization. Our data demonstrate that DGT regulates auxin transport in lateral root formation.

KEY WORDS: Auxin response, Auxin transport, Lateral root initiation, Cyclophilin A, DIAGEOTROPICA

INTRODUCTION

The formation of root branches, known as 'lateral roots', continues throughout the entire lifespan of a plant. In most eudicot plants such as *Arabidopsis* and tomato, lateral root meristems form *de novo* from cells in the pericycle cell layer of the parent root (for a recent review, see Lavenus et al., 2013a). This process comprises several distinct phases. First, some of the pericycle cells adjacent to a protoxylem pole in the basal region of the root apical meristem (also referred to as the transition zone) undergo pre-selection or 'priming' (De Smet et al., 2007; Moreno-Risueno et al., 2010). In the differentiation zone of the root, selected pericycle cells become specified as lateral root founder cells; these cells undergo asymmetric anticlinal (perpendicular to the root surface) division, giving rise to a file of short cells referred to as the stage I primordium (Malamy and Benfey, 1997). Cells in the stage I primordium divide periclinally (parallel to the root surface) to form a two-cell layered primordium (stage II). Further development generates a dome-shaped advanced primordium, then a recognizable meristem forms and the new lateral root emerges through the overlying tissues of the parent root.

A number of studies have highlighted the organogenetic power of the plant hormone auxin. Auxin biosynthesis, perception, signaling and polar transport (PAT) are all required for normal lateral root formation (reviewed by Benková et al., 2009; Lavenus et al., 2013b; Overvoorde et al., 2010; Vanneste and Friml, 2009). PAT and auxin responses are tightly interlinked and difficult to resolve *in planta* (Vieten et al., 2005). Expression of the auxin-responsive reporter gene *DR5* in vascular cells in the *Arabidopsis* root apical meristem associates with priming of adjacent pericycle cells (De Smet et al., 2007; Moreno-Risueno et al., 2010), whereas *DR5* expression in pericycle cells in the root differentiation zone of *Arabidopsis* and tomato marks their specification as lateral root founder cells (Benková et al., 2003; Dubrovsky et al., 2008; Himanen et al., 2002). Both types of *DR5* expression patterns are abolished upon application of the auxin efflux inhibitor 1-N-naphthylphthalamic acid (NPA), indicating that these auxin responses depend on PAT (De Smet et al., 2007: Himanen et al., 2002). In *Arabidopsis*, a gain-of-function mutation *solitary root* (*slr-1*/*iaa14*) leads to accumulation of a stabilized form of SLR/IAA14, a member of the Aux/IAA protein family of transcriptional repressors, and expression of mIAA14 in wild-type plants inhibits lateral root formation (Fukaki et al., 2002). A close tomato SLR ortholog is ENTIRE (E)/Sl-IAA9 (Wu et al., 2012). RNAi lines with decreased *Sl-IAA9* gene expression (Wang et al., 2005) and loss-of-function *e*/*iaa9* mutants (Zhang et al., 2007) show shoot morphological defects but normal root development.

In *Arabidopsis*, PAT relies on two major families of membrane-localized auxin efflux proteins, PIN and ABCB, and a family of auxin influx proteins, AUX1/LAX (reviewed by Vanneste and Friml, 2009). Dynamic recycling of PINs to and from the plasma membrane is essential for PIN functionality (Geldner et al., 2001; Grunewald and Friml, 2010; Kleine-Vehn et al., 2008). In the root, auxin runs from the base towards the tip (acropetal stream) and from the tip towards the base (basipetal stream). Using a self-referencing IAA-specific microelectrode that permits noninvasive continuous recordings of auxin flux rate along the root, it is possible to detect

[1]Oregon State University, Department of Botany and Plant Pathology, 2082 Cordley Hall, Corvallis, OR 97331, USA. [2]University of Fribourg, Department of Biology – Plant Biology, CH-1700 Fribourg, Switzerland. [3]Institute of Science and Technology Austria, Am Campus 1, Klosterneuburg A-3400, Austria. [4]VIB Department of Plant Systems Biology and Department of Plant Biotechnology and Genetics, Ghent University, Gent 9052, Belgium. [5]Key Laboratory of Agro-biodiversity and Pest Management of Education Ministry of China, Yunnan Agricultural University, Kunming 650201, China. [6]LINV–DIPSAA–Università di Firenze, Viale delle idee 30, Sesto Fiorentino 50019, Italy. [7]Universidad Nacional Autónoma de México, Instituto de Biotecnología, Departamento de Biología Molecular de Plantas, Apartado Postal 510-3, 62210 Cuernavaca, Morelos, México. [8]School of Life Sciences, Southwest University, Chongqing 400715, China.

*Author for correspondence (ivanchem@science.oregonstate.edu)

a distinct peak at the root transition zone (Mancuso et al., 2005; Santelia et al., 2005), correlating with a PIN-dependent auxin 'reflux loop' from peripheral towards central vascular cells (Blilou et al., 2005). Less is known about how auxin transporters are regulated by protein interactions that may influence their conformation and thus affect trafficking, stability or activity. Trafficking of ABCBs from the ER to the plasma membrane and their functionality on the membrane is maintained by the peptidyl-prolyl *cis-trans* isomerase (PPIase) FKBP42/TWD1, which does not interact with PIN auxin transporters (Bouchard et al., 2006; Wang et al., 2013; Wu et al., 2010).

Similar to FKBPs, cyclophilins (Cyps) display a PPIase activity *in vitro*, suggesting they act in protein folding (Schiene-Fischer and Yu, 2001). FKBPs and Cyps are commonly referred to as immunophilins due to their high affinity for the immunosuppressive drugs FK506 and cyclosporine A, respectively. Cyclophilin A consists of only the core PPIase domain, localizes primarily in the cytosol and nucleus, and is highly conserved from yeast to humans [reviewed by Wang and Heitman (2005)]. In higher plants, cyclophilin A has been linked to auxin-regulated development through the cloning of the *diageotropica* (*dgt*) mutation in tomato (Oh et al., 2006). DGT possesses PPIase activity and might affect plant development through physiological refolding of target proteins (Oh et al., 2006). One of the most remarkable phenotypes of *dgt* is the lack of lateral root primordium organogenesis (Ivanchenko et al., 2006). In *dgt*, the expression of members of the auxin-regulated *Aux/IAA* gene family is abnormal to a different degree, depending on organ and developmental stage (Balbi and Lomax, 2003; Mignolli et al., 2012; Mito and Bennett, 1995; Nebenführ et al., 2000). Protoplasts from *dgt* hypocotyls do not swell but instead decrease in volume when treated with auxin or antibodies against AUXIN BINDING PROTEIN 1 (ABP1), further suggesting an abnormal auxin response (Christian et al., 2003). Previous work has reported unchanged auxin transport in *dgt* root and shoot, which has led to the hypothesis that DGT regulates auxin perception or signaling but plays no role in PAT (Daniel et al., 1989; Muday et al., 1995). Here, we show that DGT is required for effective auxin transport *in planta* and in heterologous auxin-transport systems that lack plant-specific components of auxin perception and signaling. In contrast to TWD1 involved in regulation of ABCB auxin transporters, DGT appears to regulate PIN transporters.

RESULTS

The *dgt* mutant lacks auxin maxima related to pericycle cell priming and founder cell specification

We analyzed auxin signals in vascular cells in the root apical meristem related to pericycle cell priming using *DR5:GUS* and *IAA2:GUS* reporters. *DR5* was expressed in vascular cells in wild-type root tips (Fig. 1A), similar to the pattern reported in *Arabidopsis* (De Smet et al., 2007). Remarkably, vascular *DR5* signals were completely absent in *dgt*, although expression in the quiescent center region (QC) and the central root cap (columella) was present and even appeared increased compared with wild type. Treatment with the auxin transport inhibitor NPA abolished *DR5* expression in the vascular cells of wild-type roots, causing them to resemble untreated *dgt* roots. Upon a pulse treatment with IAA (5 µM for 3 h), *DR5* activity increased in the wild-type vascular cells but no expression was induced in *dgt*. On comparing the effect of a longer IAA treatment (5 µM for 40 h) with that of the synthetic auxins NAA and 2,4-D, postulated to be inefficiently transported by the auxin efflux and influx transporter, respectively (Marchant et al., 1999), we found that IAA and NAA induced multiple lateral root primordia in the wild-type root tip, whereas 2,4-D increased *DR5* expression without primordium induction. None of these treatments

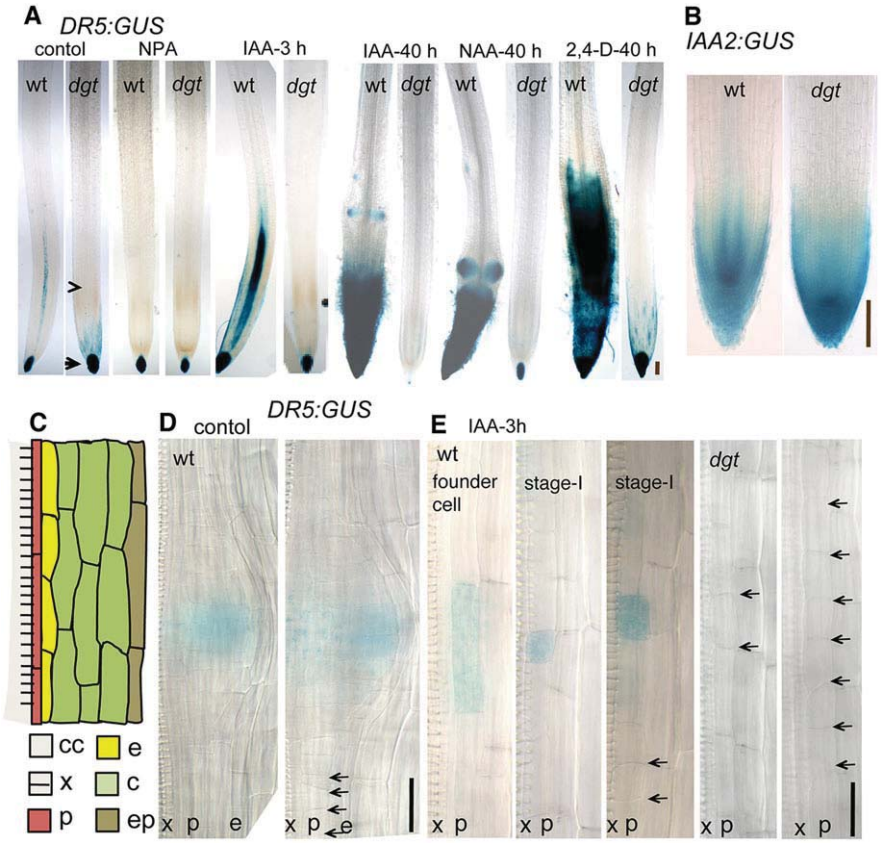

Fig. 1. The *dgt* mutant lacks auxin signals related to pericycle cell priming and lateral root organogenesis. (A) *DR5:GUS* auxin reporter expression in wild-type and *dgt* root tips after treatments as indicated. Note reporter expression in vascular cells in the wild-type root apical meristem and its absence in *dgt* (arrowhead). The *dgt* root exhibits *DR5* expression only in the QC region and central root cap (arrow). Treatment with auxin transport inhibitor NPA (10 µM for 20 h) abolishes *DR5* expression in the vascular region of wild type. Pulse treatment with IAA (5 µM for 3 h) increases *DR5* expression in stele of the wild-type root tip but has no effect on *dgt*. Treatment with IAA or NAA for 40 h induces lateral root primordia in the wild-type root tip but not in *dgt*. 2,4-D increases *DR5* expression at the root tip in wild type but not in *dgt*. (B) *IAA2:GUS* reporter expression in newly emerged lateral roots induced through meristem decapitation shows strong expression in stele of wild type and more peripheral expression in *dgt*. (C) Tomato root anatomy (one half of the root is shown). (D) Wild-type lateral root primordia showing *DR5* expression at the primordia tips. (E) The differentiation zone of wild-type and *dgt* roots after treatment with 5 µM IAA for 3 h. Arrows in D,E denote divided pericycle cells that do not show *DR5* expression. c, cortex; cc, central cylinder; e, endodermis; ep, epidermis; p, pericycle; x, xylem. Scale bars: 100 µm in A,B; 30 µm in D,E.

induced *DR5* expression in the vascular cells of *dgt* or primordium formation (Fig. 1A). Although *dgt* is unable to form lateral roots, these can be induced in both wild type and *dgt* following meristem decapitation. In induced lateral roots, which are thinner and allow for more precise tissue assessment in tomato, *IAA2* reporter expression was strong in wild-type vascular cells, whereas in *dgt* it was decreased in vascular and increased in peripheral tissues (Fig. 1B). Furthermore, upon gravitropic stimulation wild-type roots reoriented their growth direction and demonstrated asymmetric *IAA2:GUS* reporter expression on the lower side of the root, whereas *dgt* roots did not reorient, and did not show asymmetric *IAA2:GUS* expression (supplementary material Fig. S1). Thus, *dgt* root tips displayed spatial abnormalities in auxin reporter expression that could be justifiably interpreted as resulting from a defect in PAT.

We next analyzed auxin signals in pericycle cells in the *dgt* root differentiation zone. The tomato root anatomy is similar to that of *Arabidopsis* except that the cortex has three cell layers instead of one (Fig. 1C). In the differentiation zone of the wild-type root, *DR5* was expressed in lateral root primordia and increased at the primordia tips (Fig. 1D). It appears that in tomato, some primordia are initiated by relatively longer stretches of divided pericycle cells but those extra cells do not show *DR5* expression and do not participate in further primordium development (Fig. 1D, arrows). Because, in tomato, *DR5* expression was insufficiently strong at early stages of primordium organogenesis, we analyzed roots that were pulse-treated with IAA for 3 h (Fig. 1E). In these roots, *DR5* expression/signal was clearly seen in founder cells and stage I primordia in wild type, apparently associated with primordia centers and absent from short pericycle cells at the primordia periphery. In *dgt*, no *DR5* expression was observed in this zone. Although some *dgt* roots exhibited short pericycle cells apparently resulting from anticlinal pericycle cell division, these cells did not show *DR5* expression (Fig. 1E). We conclude that, in tomato, *DR5* marks auxin signals associated with primordium initiation and growth; however, such signals are absent in *dgt*.

To confirm that *DR5* expression in vascular cells at the wild-type tomato root tip is indeed related to the process of pericycle cell priming, as has been shown in *Arabidopsis*, we treated seedlings with a 3 h pulse of IAA, transferred them onto fresh agar plates, and marked the position of the root tips. As roots elongated below the mark, the *DR5*-positive vascular tissues remained just above the mark. Analysis of the root zone above the mark in a time course revealed *DR5* activity in pericycle cells 20 h after the treatment, and a few hours later a primordium formed, then a lateral root emerged (Fig. 2). However, no primordium organogenesis or lateral root formation was observed in *dgt*, consistent with the lack of *DR5* response in vascular cells of the root apical meristem (Fig. 2).

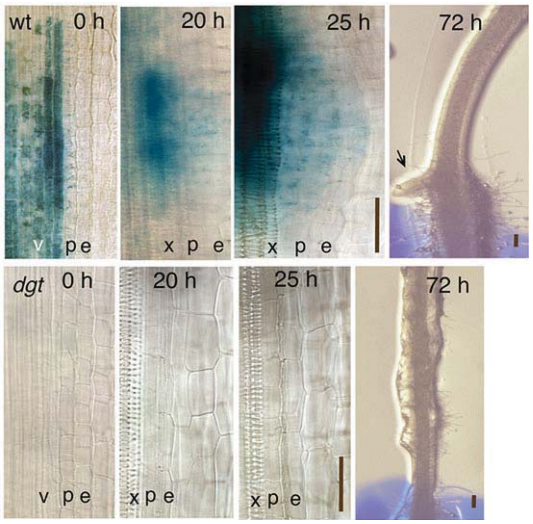

Fig. 2. Induction of lateral root organogenesis after treatment with 5 µM IAA for 3 h. At '0' h post-treatment, *DR5* expression is increased in developing vascular cells in the wild-type root tip, but is not observed in *dgt*. At 20 h, adjacent pericycle cells demonstrate *DR5* expression and primordium formation in wild type, and at 72 h a lateral root is formed; this process does not take place in *dgt* roots. Panels (0-25 h) show images from cleared roots; panels (72 h) show live roots on agar plates. e, endodermis; p, pericycle; v, vascular cells; x, xylem. Scale bars: 50 µm (0, 20 and 25 h); 100 µm (72 h).

DGT tissue-specific expression and subcellular localization

DGT:GUS expression was observed in roots, cotyledons and leaves, and is apparently associated with the vasculature in these tissues (Fig. 3A-C). *DGT* activity was broader in cross-sections through the middle part of the meristem (Fig. 3D), but was restricted to the central cylinder and pericycle and endodermis near the transition and elongation zone, where it was observed predominantly at the phloem poles (Fig. 3E). At the beginning of the differentiation zone, some *DGT* expression was also detected in early-stage lateral root primordia (Fig. 3F). To observe the subcellular localization of DGT in pericycle cells, we stably expressed a *DGT*:mCherry-DGT fusion in *Arabidopsis*, which has thinner roots that are amenable to confocal microscope imaging of inner tissues. Consistent with the *DGT:GUS* expression in tomato, mCherry-DGT fluorescence was observed in lateral root founder cells and lateral root primordia in *Arabidopsis* roots (Fig. 3G). At the subcellular level, DGT was observed in the nucleus and the cytoplasm in early-primordia cells, consistent with the subcellular localization of yeast and mammalian cyclophilin A (reviewed by Wang and Heitman, 2005). Transformation the *DGT:mCherry-DGT* construct into *dgt* restored the lateral root formation defect, demonstrating the functionality of the mCherry-DGT fusion (supplementary material Fig. S2). The DGT expression pattern supports participation in lateral root primordium organogenesis and suggests a nuclear and a cytoplasmic function of DGT.

DGT and E/SlI-IAA9 pathways overlap partially

Transformation of the *Arabidopsis IAA14:mIAA14-GFP* construct in tomato resulted in a dramatic reduction in lateral root formation (Fig. 4A) similar to that observed in *Arabidopsis* (Fukaki et al., 2002), indicating conservation of the SLR-governed pathway in tomato. To test whether DGT genetically interacts with the tomato SLR ortholog E, we generated a *dgt e* double mutant. Lateral root formation was partially restored in the *dgt e* background, although the appearance of root branches was much delayed (Fig. 4B). Comparing the primordium development, we found that wild-type and the *e* single mutant roots exhibited primordia of all stages, *dgt* roots rarely exhibited primordium initiation, and *dgt e* roots predominantly exhibited structures resembling stage I primordia (Fig. 4C). On exposure to 5 µM IAA for 40 h, the wild type and the *e* mutant roots formed lateral root primordia close to the root apex as expected, whereas *dgt* and the *dgt e* double mutant were equally insensitive to the treatment (Fig. 4D). Thus, downregulation of *E* partially restored the primordium initiation in *dgt* but not the primordium outgrowth and the ability to respond to exogenously applied auxin.

Grafting of a wild-type shoot partially restores the lateral root defect in *dgt*

Because shoot-derived auxin is known to stimulate the outgrowth of lateral root primordia in *Arabidopsis* (Bhalerao et al., 2002), and application of the auxin transport inhibitor NPA was shown to

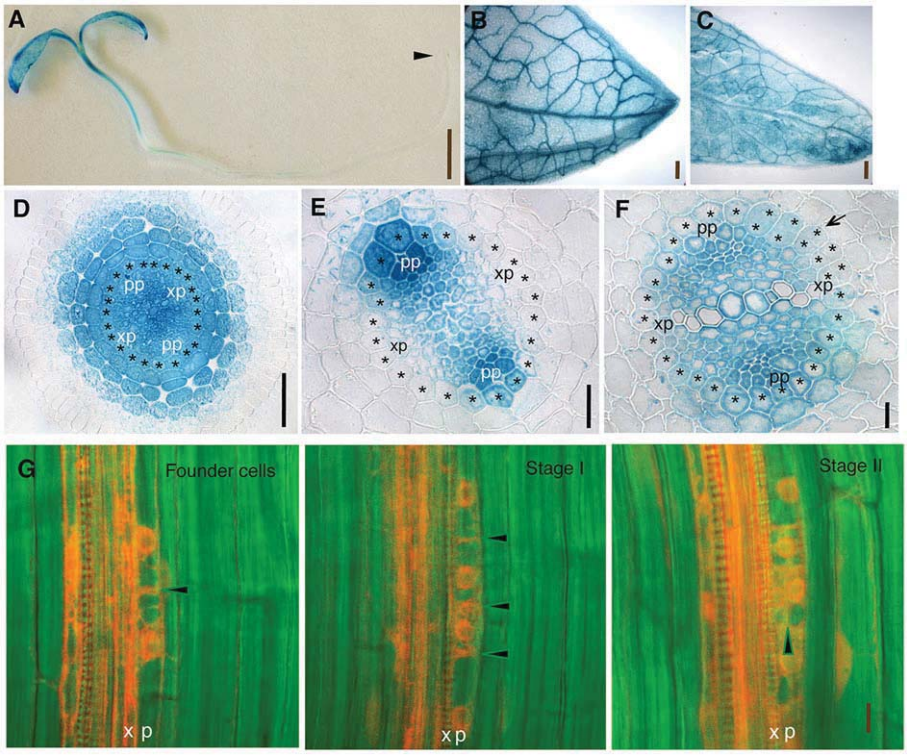

Fig. 3. DGT expression pattern and subcellular localization. (A-F) Expression of *DGT:GUS* reporter in tomato. (A) Five-day-old seedling, (B) cotyledon, (C) leaf-1 primordium, (D-F) cross-sections through the middle of the meristem (D), transition zone (E) and the beginning of the differentiation zone (F) of an 8-day-old seedling. Asterisks indicate the pericycle cell layer and an arrow indicates an early primordium. pp, phloem pole; xp, xylem pole. (G) Expression of *DGT:mCherry-DGT* construct in *Arabidopsis*. p, pericycle; x, xylem. Scale bars: 5 mm in A; 300 μm in B,C; 50 μm in D-F; 20 μm in G.

inhibit lateral root formation (Reed et al., 1998), we tested whether grafting of a wild-type scion would improve the lateral root formation in the *dgt* rootstock. Seedlings were grafted at the middle of the hypocotyl as soon as they germinated. At this stage, neither wild type nor *dgt* had root branches, and the primary wild-type root had on average seven primordial, whereas primordia were very rare in *dgt*. Older soil-grown *dgt* plants also had root systems much smaller than those in wild type. Grafted seedlings were analyzed for root development at 12 days post-grafting (Fig. 5). As expected, root development was minimal in self-grafted *dgt* seedlings compared with self-grafted wild-type plants (Fig. 5A). The grafting of a *dgt* scion onto a wild-type rootstock did not affect the root development. However, when a wild-type scion was grafted onto a *dgt* rootstock, the development of the *dgt* rootstock was significantly improved, confirming an earlier report (Zobel, 1973). Histological markers in the differentiation zone were improved, including asymmetric pericycle cell division, early-stage primordium formation and *DR5* expression in primordia (Fig. 5B). At the root tip, *DR5* expression was missing in vascular cells of self-grafted *dgt* plants, and was restored in some of the plants with a *dgt* rootstock grafted on a wild-type shoot (Fig. 5C). Furthermore, root growth in a *dgt1-1* (AC background) rootstock was restored upon grafting of an ethylene overproducing *Epinastic* (*Epi*) mutant scion (VFN8 background) and *e* mutant scion (AC background) but not *dgt-dp* (Chatham background), indicating that the effect was a property of the DGT protein and not the genetic background used for grafting (supplementary material Fig. S3). Thus, grafting improved the auxin responses and lateral root formation in the *dgt* rootstock, consistent with participation of a mobile signal. We therefore tested whether DGT could move from the shoot into the root in grafted plants. An *Arabidopsis* cyclophilin A antibody (Lippuner et al., 1994) detects DGT in wild-type tissues but not in *dgt* tissues in western blots (Oh et al., 2006). Using this antibody, we could not detect any DGT signal in *dgt* rootstocks grafted on wild-type scions (n=5 plants) (supplementary material Fig. S4), ruling out the possibility that DGT movement restored the lateral root formation in grafted *dgt* rootstocks.

Measurements of auxin transport detect abnormal PAT fluxes in *dgt*

To investigate defects in PAT in *dgt*, transport of radiolabelled IAA was assayed. Root IAA transport from the root-shoot junction to the root tip (root-ward) was increased in *dgt* (Fig. 6A), whereas transport from the root tip toward its base (shoot-ward) was decreased (Fig. 6B). By comparison, movement of benzoic acid (BA), assayed as a diffusion control, was unchanged between *dgt* and wild type (Fig. 6A,B). Using an IAA-specific microelectrode, we then analyzed the IAA influx velocity along the root tip. In wild type, the transition between the meristem and elongation zone was at 0.85±0.06 mm from the root apex; in *dgt* it was at 0.58±0.04 mm (Fig. 6C). An IAA influx peak averaging 188 fmoles cm^{-2} s^{-1} was recorded in this zone in wild type that was dramatically reduced to 106 fmoles cm^{-2} s^{-1} in presence of NPA, as expected (Fig. 6C,D). In *dgt*, the IAA influx peak averaged only 98 fmoles cm^{-2} s^{-1}, comparable to that in NPA-treated wild-type roots, and even more strikingly was completely unaffected by the presence of NPA (Fig. 6C,D). Thus, the *dgt* root tip seems to be inefficient in generating an IAA reflux loop at the transition zone and supplying auxin into vascular cells involved in lateral root formation.

Modulating the DGT level results in changes in cellular IAA efflux, and subcellular localization and functionality of PIN auxin transporters

Protoplasts prepared from *dgt* leaves had an increased IAA efflux compared with wild type, indicating that DGT is a negative PAT regulator at the cellular level (Fig. 7A). To separate the effect of DGT on PAT from that on auxin signaling, we then used a yeast (*Saccharomyces cerevisiae*) auxin-transport system. HA-DGT had no effect on its own, but reduced *Arabidopsis* PIN2-driven and synergistic ABCB1/PIN1-mediated IAA efflux, apparently acting

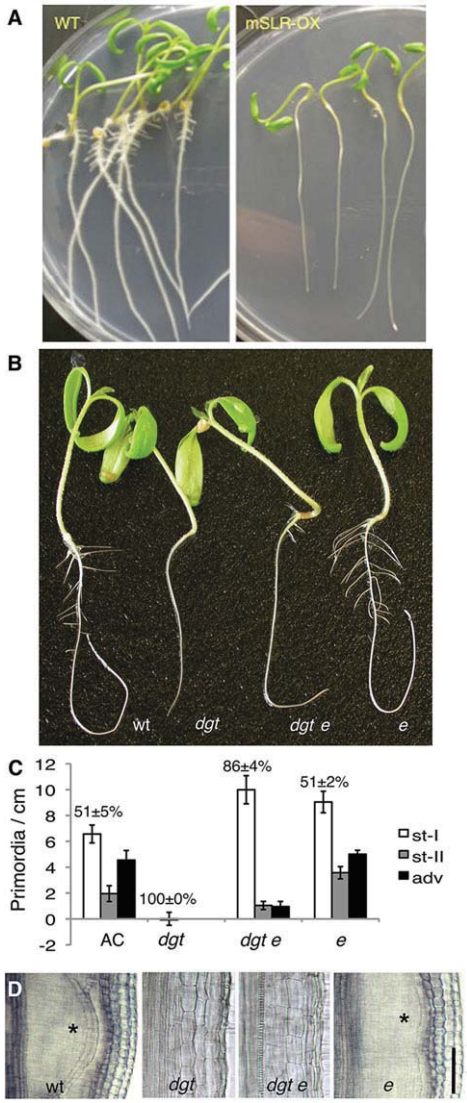

Fig. 4. Partial overlap between DGT and ENTIRE (E)/Sl-IAA9 pathways. (A) Inhibition of lateral root formation in tomato upon expression of *Arabidopsis IAA14:mIAA14-GFP* construct. (B) Comparison of wild-type and mutant phenotypes. Lateral root formation is partially restored in *dgt e* mutant compared with *dgt*. (C) Quantification of primordia stages: ~3-cm-long root apices were excised from each genotype and primordia quantified after root clearing. The percentages of stage I primordia are indicated. Only two primordia, both from stage I, were found in 20 *dgt* roots. Data are mean±s.e.m. (D) Inability of *dgt* and *dgt e* mutants to form primordia upon treatment with IAA (5 µM for 40 h). Morphogenesis of primordia in the transition zone in wild type and *e* is marked with asterisks. The larger cell size in *dgt* and *dgt e* indicates that the IAA treatment did not suppress cell elongation in these genotypes. Scale bar: 30 µm in D.

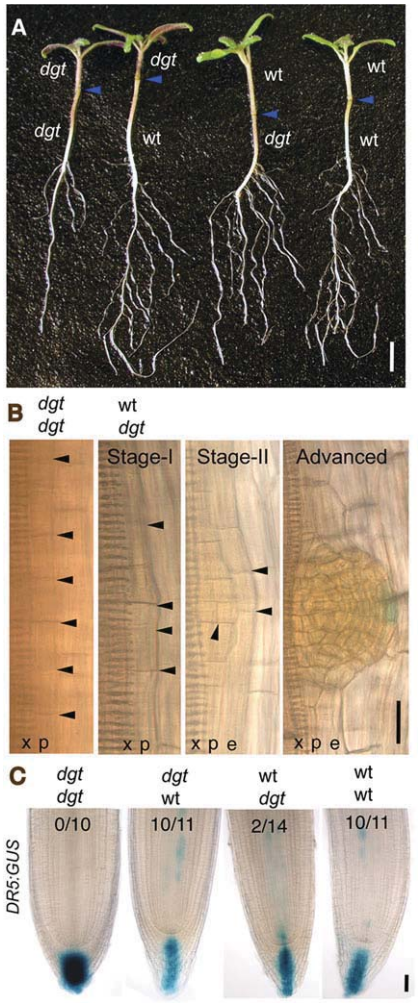

Fig. 5. Grafting of a wild-type shoot partially restores development in the *dgt* rootstock. (A) Root system phenotypes in grafted tomato seedlings. Arrowheads indicate the sites of the graft junctions. The tissue identity is indicated. (B) Improvement of primordium organogenesis in *dgt* roots upon grafting of a wild-type scion. (C) *DR5* expression in root tips of grafted plants. *n* (*dgt*/*dgt*)=10 roots from eight plants, *n* (*dgt*/wt)=11 roots from three plants, *n* (wt/*dgt*)=14 roots from five plants, *n* (wt/wt)=11 roots from three plants. The number of roots with *DR5* expression in vascular tissues is indicated. Scale bars: 10 mm in A; 30 µm in B; 50 µm in C.

in line with the above-described function as a negative regulator of auxin efflux (Fig. 7B). HA-DGT had no significant effect on ABCB1 alone (Fig. 7B), indicating that DGT might act preferably as a negative regulator of PIN transporters. Because PIN1 is not functional in *S. cerevisiae* without ABCB1 (Blakeslee et al., 2007; Kim et al., 2010), we re-tested the effect of DGT on PIN1 in a tobacco (*Nicotiana benthamiana*) leaf transport system (Henrichs et al., 2012). Analogous to the yeast system, a mCherry-DGT fusion had a negative effect on PIN1-driven IAA efflux but no significant effect on ABCB1-driven IAA efflux, demonstrating a preferential regulation of PIN transporters (Fig. 7C).

TargetP searches (at http://www.cbs.dtu.dk/services/TargetP/) did not reveal any canonical subcellular localization signals in DGT, with the exception of a potential palmitoylation signal at the C terminus; such signals are important for protein targeting to the plasma membrane and/or interactions with membrane proteins. To explore how DGT could functionally affect auxin transporters, we analyzed the colocalization of DGT with *Arabidopsis* PIN1 and ABCB1 upon co-expression in *N. benthamiana* leaves. When expressed alone, DGT localized predominantly in the nucleus, in addition to signals in the cytoplasm and the cell periphery as expected; PIN1 and ABCB1 localized predominantly to the plasma membrane, consistent with previous results (Henrichs et al., 2012) (Fig. 7D). When DGT was co-expressed with ABCB1, the localization of ABCB1 did not change significantly, but most of the DGT signal disappeared from the nucleus and appeared on the cell periphery (Fig. 7E), suggesting that ABCB1 may directly or indirectly affect localization and putative nuclear and cytoplasmic function of DGT. When DGT was co-expressed with PIN1, the localization of both proteins was modified:

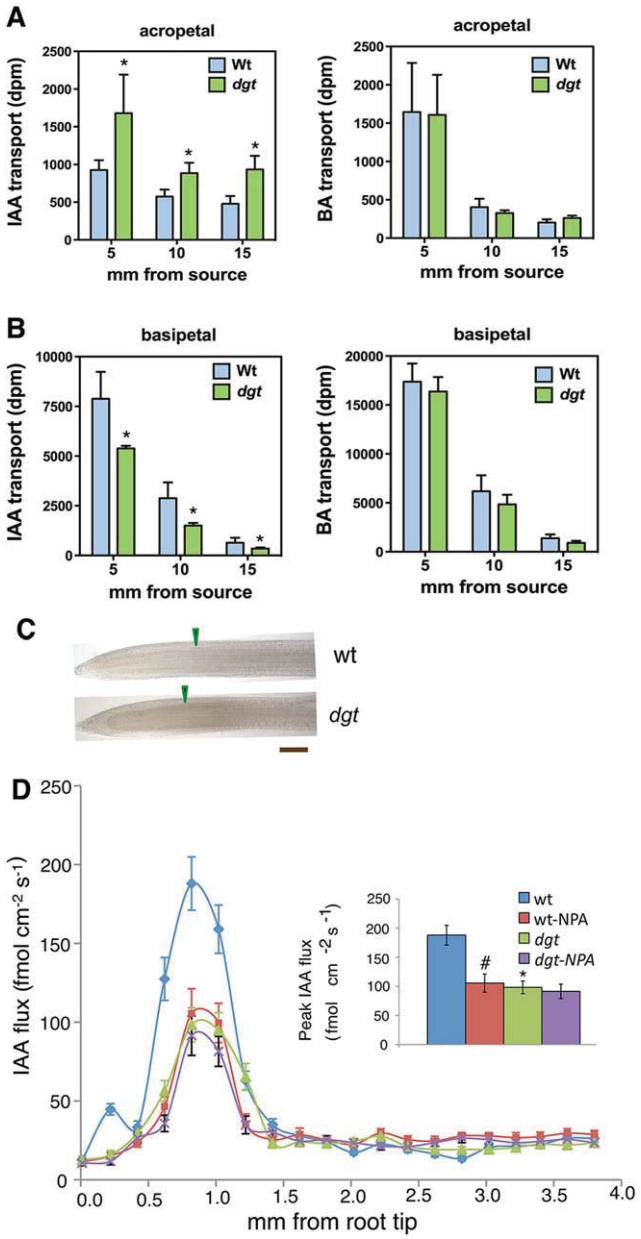

Fig. 6. *dgt* roots show defects in polar auxin transport. (A,B) Acropetal (A) and basipetal (B) IAA and benzoic acid (BA) transport in wild-type (wt) and *dgt* roots. IAA and BA radioactivity sections 5-10 mm (5), 10-15 mm (10) and 15-20 mm (15) from the source; data are mean±s.e.m. (n=4). (C) Images of a wild-type and a *dgt* root; arrowheads indicate the length of the meristem. (D) IAA influx profiles and peak influx rates (inset) along wild-type (wt) and *dgt* root tips in the absence and presence of NPA. Data are mean±s.e.m. (n=12). Asterisk indicates statistically significant differences between genotypes; # indicates statistically significant differences between treatments ($P \leq 0.01$, t-test). Scale bar: 50 µm.

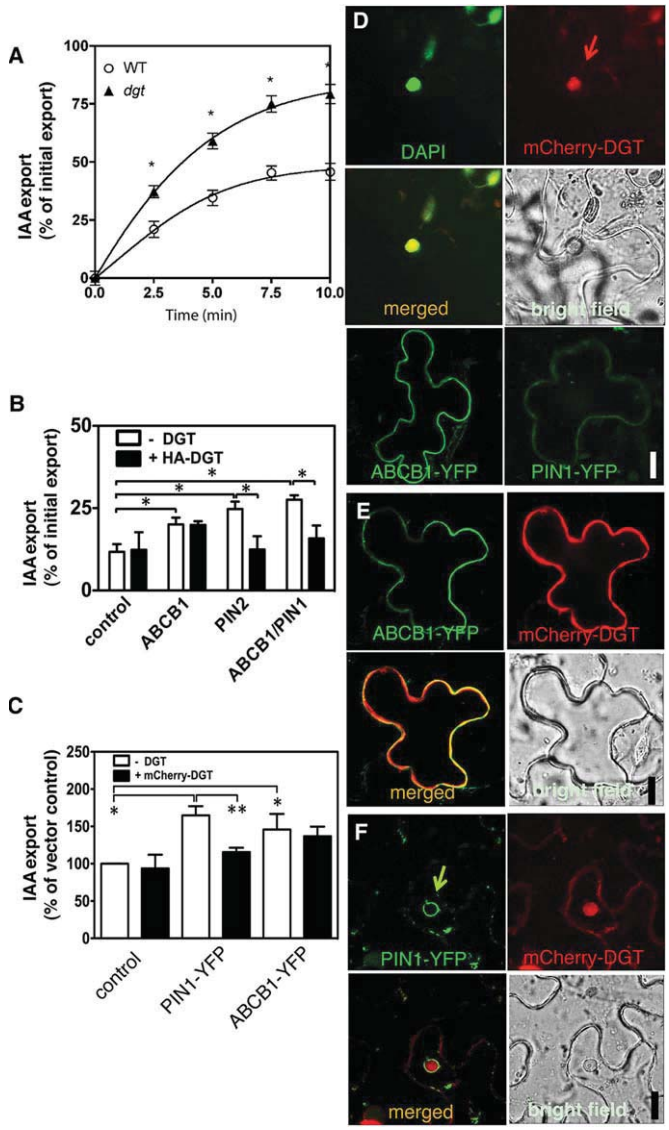

Fig. 7. Effect of DGT expression level on PIN- and ABCB-mediated auxin efflux. (A) dg*t* leaf protoplasts exhibit increased IAA export (mean±s.e.m.; n=4). (B) Co-expression of DGT blocks *Arabidopsis* PIN2 and synergistic PIN1/ABCB1 IAA export in yeast (mean±s.e.m.; n=4). PIN1 is inactive in the absence of ABCB1 in the yeast *S. cerevisiae*. (C) Co-transfection of *N. benthamiana* leaves with mCherry-DGT significantly reduces *Arabidopsis* PIN1 but not ABCB1 IAA export activity. IAA efflux was calculated relative to the initial export, where vector control was set to 100% (mean±s.e.m.; n=4). (D) Single transfection results in nuclear and weak cytoplasmic and PM labeling (arrow) for mCherry-DGT and PM locations for ABCB1-YFP and PIN1-YFP, respectively. (E,F) Co-transfection of mCherry-DGT does not alter ABCB1-YFP location (E) but shifts PIN1-YFP to the nuclear periphery (F, arrows). Both ABCB1 (E) and PIN1 co-expression (F) enhance mCherry-DGT presence at the cell periphery. Typical results from four independent experiments are shown in each case. (A-C) Significant differences (unpaired t-test with Welch's correction, P<0.05) are indicated by asterisks. Scale bars: 20 µm.

a significant proportion of PIN1 shifted from the plasma membrane to the nuclear periphery, whereas DGT increased on the cell periphery (Fig. 7F). The PIN1 internalization following DGT co-expression explains the negative effect of DGT on PIN-driven auxin efflux, and the lack of DGT effect on ABCB1 localization is in line with unchanged ABCB1-driven auxin efflux (Fig. 7B,C). Together, the data supported a function of DGT in PAT that was independent of auxin signaling, and identified distinct interactions of DGT with different types of auxin transporters.

DGT affects PIN expression and localization to the plasma membrane at the root tip

We analyzed the expression of *PIN* mRNAs in the apical 1 cm region of the root. We found no significant change in tomato *PIN1a, b* levels, whereas the expression of *PIN2* was reduced (Fig. 8A). We also analyzed the PIN protein behavior using *Arabidopsis* PIN1 and PIN2 antibodies. Tomato PIN1 and PIN2 showed a typical polar

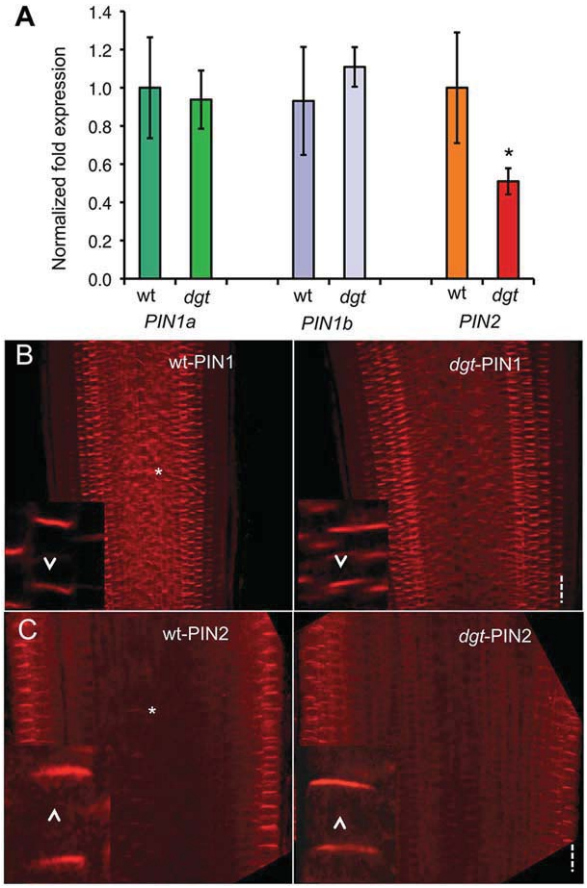

Fig. 8. PIN expression and plasma membrane localization in *dgt* root tips. (A) Relative expression of tomato *PIN1a*, *PIN1b* and *PIN2* mRNA in root tips of wild-type and *dgt* seedlings (combined values from three experiments performed in duplicate). Data are mean±s.e.m., $P<0.01$. (B) Immunodetection of tomato PIN1 in root tips of wild type and *dgt* (arrowheads). (C) Immunodetection of tomato PIN2 in root tips of wild type and *dgt* (arrowheads). PIN2 signal is more condensed in *dgt* compared with wild type. PIN signals are present in stele of wild-type roots (asterisks) but absent in *dgt*. Representative images are from four independent experiments with total of 60 roots per group. Scale bars: 50 µm in B; 75 µm in C.

localization known from *Arabidopsis*, with PIN1 localizing on the lower/rootward face of cells in central tissues, and PIN2 on the upper/shootward face of cells in more peripheral tissues (Fig. 8B,C). Notably, PIN1 signals were essentially missing in stele tissues at the *dgt* root tip (Fig. 8B). We could not assess the PIN1 plasma membrane localization in those cell files due to the low expression level. In the cell files where PIN1 was normally present its plasma membrane localization appeared normal (Fig. 8B, inset). By contrast, PIN2 plasma membrane localization was modified showing a notably broader localization domain with 'fuzzy' appearance in the wild type when compared with a narrow more-compact signal in *dgt* (Fig. 8C, inset). The PIN2 signal distribution along the membrane (measured in pixels) was similar in wild type and *dgt* (17.2±2.7 vs. 16.2±3.3, respectively) but the distribution of the signal across the plasma membrane reached 5.0±1.4 in wild type and only 2.4±0.9 in *dgt* (P=6.17519E-36; mean±s.d.; n=266 cells from 13 roots in wild type and 191 cells from eight roots in *dgt*). In the wild type, the mean PIN2 signal intensity at the plasma membrane was 60.64±0.9043 and inside the cell it was 51.12±0.8276 (ratio inside/PM: 0.8446), whereas in the *dgt* roots the PIN2 signal at the membrane was 54.55±1.099, and inside the cell it was 42.22±0.9123 (ratio inside/PM: 0.7663). Thus, the PIN2 signal in *dgt* roots was overall lower but more sharply defined at the plasma membrane, and the proportion of PIN2 allocated to the plasma membrane was significantly higher (P<0.05).

In an attempt to analyze the subcellular trafficking of PIN2, we also tried treatments with the trafficking inhibitor BFA that in *Arabidopsis* interferes with the constitutive endocytic recycling of PIN proteins to the plasma membrane and leads to PIN internalization (Geldner et al., 2001; Kleine-Vehn et al., 2008). The BFA treatment in tomato roots was ineffective as we did not see the typical 'BFA compartments' with internalized PIN proteins, as observed in *Arabidopsis*, presumably due to different arrangements of BFA-sensitive and -insensitive ARF GEFs in tomato when compared with *Arabidopsis*. Altogether, the results show that the *dgt* mutation affects the *PIN* expression domain and expression level, as well as the plasma membrane localization of PIN proteins.

DISCUSSION

Our results show that DGT is required for the generation of PAT-driven auxin maxima that are essential for lateral root formation. Two earlier works reported unchanged PAT in *dgt* (Daniel et al., 1989; Muday et al., 1995). However, it is important to note that both studies detected increased transport of radiolabelled IAA in *dgt* hypocotyls (Daniel et al., 1989, Fig. 2) and from the root base towards the root tip (Muday et al., 1995, Fig. 8) but interpreted this as 'normal'. We observed increased root transport from the root-shoot junction to the root tip and decreased transport from the root tip toward the root base, demonstrating clearly abnormal PAT fluxes and explaining our earlier findings of increased auxin level and abnormal distribution along the *dgt* root tip (Ivanchenko et al., 2006). Although more auxin moves from the aerial parts of *dgt* into the root, it is abnormally distributed and no response maxima occur in stele tissues related to lateral root initiation. Low auxin supply into the stele of *dgt* is evident from low expression of auxin-responsive *DR5*, *IAA2* and *PIN1* signals, and inability of the *e/sl-iaa9* mutation to restore the outgrowth of lateral root primordia. The increased PAT in the *dgt* shoot might result from increased cellular efflux, occur in response to PAT deficiencies in the root, or be related to a putative yet unknown function of DGT in leaves, whereas the decreased basipetal PAT at the root tip correlated with decreased expression of *PIN2*.

The root tip is the most dynamic root region with respect to PAT. In the tip, auxin is moved down the vascular tissues mainly by PIN1, and redirected at the transition zone from peripheral into vascular tissues in a 'reflux loop' by PIN2, PIN3 and PIN7, providing stable auxin circulation through the meristem (Blilou et al., 2005). The IAA influx peak recorded at the *dgt* transition zone with an IAA-specific microelectrode was reduced to 50% and was insensitive to NPA, a potent auxin-efflux inhibitor, consistent with inefficient IAA supply into vascular cells. This defect was much greater than those reported in loss-of-function *Arabidopsis twd1* mutant (Bouchard et al., 2006; Wang et al., 2013) and *pin2* mutant in blue light conditions (Wan et al., 2012), the peaks of which average at ~80% of wild type. The more severe *dgt* phenotype argues that multiple transporters, PIN1, PIN2, and potentially also PIN3 and PIN7, might be regulated by DGT.

We also observed that grafting of a wild-type scion partially rescued the auxin response in the root tip vasculature of the *dgt* rootstock, leading to primordium initiation, and antibodies did not detect DGT movement into the rootstock. We therefore hypothesize that the rescue was achieved through improving auxin transport from the wild-type scion. A recent study in *Arabidopsis* has shown

that radiolabelled auxin moves down the vasculature from the shoot through plasmodesmal connections in the phloem and accumulates at the root tip, but that the signal is barely perceptible in NPA-treated plants, demonstrating a strong dependence on PAT (Bishopp et al., 2011). Thus, the simplest explanation of our grafting results is that in the grafted wild-type scion, auxin is more successfully channeled into the vasculature, allowing for movement into the vasculature of the *dgt* rootstock. Auxin transport from developing true leaves has been reported to stimulate the emergence of lateral root primordia (Bhalerao et al., 2002), whereas basipetal PAT from the root tip has been proposed to stimulate the primordium initiation (Casimiro et al., 2001). Our results show that, at least in tomato, the shoot is important for root primordium initiation.

In contrast to the *Arabidopsis* immunophilin TWD1, which has been demonstrated to act as a positive regulator of ABCB-driven auxin efflux (Bouchard et al., 2006; Wang et al., 2013; Wu et al., 2010), our functional studies implicate DGT as a negative regulator of auxin efflux that preferentially affects PIN transporters at the cellular level. First, protoplasts from *dgt* leaves displayed an increased IAA efflux, whereas overexpression of DGT in tobacco leaves reduced the PIN-mediated IAA efflux. Second, in a yeast-based auxin-transport system, which lacks plant-specific auxin responses, DGT co-expression still reduced the PIN-mediated IAA efflux, providing strong evidence that DGT affects PIN functionality independently of auxin signaling. As to how DGT could affect auxin transporters at the protein level, DGT reduced the PIN1 plasma membrane localization simultaneously with reducing the PIN1-mediated auxin efflux upon co-expression in tobacco leaves. This result agrees with previous observations in *Arabidopsis* showing that increasing PIN levels at the plasma membrane leads to elevated auxin efflux (Paciorek et al., 2005; Robert et al., 2010). Furthermore, the proportion of PIN2 on the plasma membrane versus inside the cell was also increased at the *dgt* root tip and displayed a sharper signal when compared with wild type. Together, the data demonstrate that DGT is implicated in a mechanism related to membrane localization of PINs. However, both PIN1 and ABCB1 were also able to modify the subcellular localization of DGT upon co-expression in tobacco leaves, suggesting complex inter-relationships among all three types of proteins. Whether DGT interacts with PINs (and ABCBs) directly or via other proteins or molecules remains to be determined. Given that the gene transcription of *DGT* is downregulated by auxin at the root tip (Ivanchenko et al., 2013), that *PIN* expression is upregulated in *Arabidopsis* (Vieten et al., 2005), and PIN and ABCB activities interact synergistically (Blakeslee et al., 2007), one can envision an extremely complex functional feedback between DGT level, auxin level, functionality and membrane localization of PINs, and maintenance of PAT fluxes at the plant level. This complexity is evident in the observed complex effect of the *dgt* mutation on the expression levels of the *PIN* genes and their expression domain, and on PIN protein localization to the plasma membrane at root tip.

It has been shown that mutations in the rice cyclophilin gene *OsCYP2* cause a similar inability to form lateral roots (Kang et al., 2013; Zheng et al., 2013) and mutations in the *DGT* ortholog in the moss *Physcomitrella patens* cause auxin-resistant phenotypes (Lavy et al., 2012), demonstrating a conservation of DGT-like function in auxin-regulated development. Several aspects of cyclophilin A function have also emerged in non-plant systems, suggesting it to be a multifunctional protein. Cyclophilin A has been linked to regulation of protein activity (Brazin et al., 2002; Colgan et al., 2004), protein interactions (Zander et al., 2003; Sorin and Kalpana, 2006) and protein trafficking (Ansari et al., 2002; Galigniana et al., 2004). Another suggested function of yeast and mammalian cyclophilin A is regulation of gene expression at the level of chromatin folding (Arévalo-Rodríguez et al., 2000; Pijnappel et al., 2001; Arévalo-Rodríguez and Heitman, 2005; Lu et al., 2006). Our findings demonstrate a role of a plant cyclophilin A in polar auxin transport. Some phenotypes of the *dgt* mutant cannot be directly explained by a defect in auxin transport, e.g. the inability of *dgt* to respond to exogenously applied auxin with increased *DR5* auxin reporter expression at the root tip, and the partial restoration of lateral root formation by a loss of ENTIRE (IAA9). Therefore, in addition to affecting auxin-regulated gene expression via regulating PAT, DGT could also have a direct effect on auxin signaling, or even act more broadly on gene expression, possibilities suggested by the nuclear expression of DGT. In addition, the *dgt* root tip shows an increased level of hydrogen peroxide (H_2O_2) (Ivanchenko et al., 2013), and this oxidative environment could contribute to decreasing the auxin sensitivity of *dgt* due to auxin oxidation, to which grafted plants might be less susceptible because of the direct auxin delivery into vascular tissues.

MATERIALS AND METHODS

Plant material and growth conditions

Wild-type tomato (*Solanum lycopersicum*), *dgt1-1* and *entire* (*e*) mutants in the Ailsa Craig (AC) background, and *Arabidopsis* seedlings in the Columbia 0 (Col) background were used unless otherwise stated. The *dgt1-1* and *dgt-dp* tomato mutant alleles (Oh et al., 2006), the *e* mutant (Zhang et al., 2007), *Epi* mutant (Fujino et al., 1988), transgenic tomato *DR5:GUS* line (Dubrovsky et al., 2008), tomato *IAA2:GUS* line (Dubrovsky et al., 2011) and *IAA14:mIAA14-GFP* construct (Fukaki et al., 2002) have been reported. Tomato and *Arabidopsis* seedlings were grown in 0.2× MS agar medium with vitamins (PhytoTechnology). Indole-3-acetic acid (IAA) (Sigma), N-naphthalene-acetic acid (NAA) (Sigma), 2,4-dichloro phenoxyacetic acid (2,4-D) (Sigma) and NPA (Chem Service) were used at concentrations and exposure times as indicated. For grafting, tomato seedlings were germinated in vermiculite moistened with 0.2× MS liquid medium and grafted as described in *Arabidopsis* (Turnbull et al., 2002).

Cloning procedures and plant transformation

For the *DGT:GUS* construct, the 5′ flanking region of the *DGT* gene from −1389 to +36 bp was cloned between the *Kpn*I and *BamH*I sites in a pCAMBIA1300 vector (http://www.cambia.org), and the GUS-coding sequence between the *BamH*I and *Sal*I sites. A TGA stop codon was introduced at the end of GUS. For the *DGT:mCherry-DGT* construct, the 5′ region of the *DGT* gene was cloned between the *Hin*dIII and *Sal*I sites of pCAMBIA1300, and an mCherry-DGT in-frame fusion was introduced between the *Sal*I and *Bam*HI sites. For expression in *N. benthamiana* leaves, the mCherry-DGT fusion was amplified by PCR and cloned under 35S constitutive promoter between *Bam*HI and *Spe*I sites in pCB302-3. For yeast expression, HA-DGT fusion was generated by PCR and cloned between *Bam*HI *and Sal*I sites in pRS314CUP. *Arabidopsis* transformation was performed by the floral dip method, and tomato transformation as described previously (Ivanchenko et al., 2006).

Histological analyses and microscopy

GUS staining was performed as described previously (Ivanchenko et al., 2006) and western blot as described previously (Oh et al., 2006). For meristem and lateral root primordium analyses, roots were cleared as described previously (Malamy and Benfey, 1997), and mounted in saturated chloral hydrate solution in 10% glycerol. For tissue sectioning, roots stained for GUS were imbedded in Technovit 7100 (Electron Microscopy Sciences). Root samples were analyzed under a Zeiss Axiovert microscope with differential interference contact (DIC) optics. Confocal microscopy in *Arabidopsis* roots and *N. benthamiana* leaves was performed using an inverted Zeiss LSM 510 Meta (Carl Zeiss) microscope with ×63 (NA 1.2, C-Apochromat) objective with water immersion.

Auxin transport assays

Root acropetal (root-shoot junction to root tip) and basipetal (root tip to root base) PAT measurements were performed as described previously (Lewis and Muday, 2009). Continuous recordings of IAA fluxes at the root apex with a self-referencing IAA-specific microelectrode were performed as described previously (Mancuso et al., 2005). For NPA response, plants were treated with or without 5 µM NPA for 2 h. Yeast IAA transport was performed as described previously (Kim et al., 2010). Relative export from yeast is calculated from retained radioactivity as follows: (radioactivity in the yeast at time t=10 min)−(radioactivity in the yeast at time t=0)×(100%)/(radioactivity in the yeast at t=0 min); mean values from four independent experiments are presented. IAA export from *N. benthamiana* leaf tissue was analyzed as described previously (Mravec et al., 2009; Henrichs et al., 2012). Tomato protoplast assays were conducted as for tobacco, except that enzyme digestion was performed overnight at room temperature. Relative export from protoplasts is calculated from exported radioactivity as follows: (radioactivity in the protoplasts at time t=x min)−(radioactivity in the protoplasts at time t=0)×(100%)/(radioactivity in the protoplasts at t=0 min); mean values from four independent experiments are presented.

Quantification of *PIN* mRNA expression

RT-qPCR was performed as described previously (Ivanchenko et al., 2013). Primers for tomato PIN1a (Bayer et al., 2009), PIN1b (Acc. HQ127074) and PIN2 (Acc. HQ127077) were designed to include part of the 3′ UTRs: PIN1a F 5′-AGCACAGGGGTCATATTTGG, R 5′-TCCCAACAATTG-ACCATTCA; PIN1b F 5′-TCCTGACATTCTTAGCACAGC, R 5′-TTTA-TCTCCATGCCAATTGCT; PIN2 F 5′-CAGGACCAGCTGTTATTGCT, R 5′-CCAAGTCTACACACCAAGAAGC.

Analyses of PIN expression at the root tip

Roots from 8-day-old tomato seedlings were probed with *Arabidopsis* anti-PIN1 or -PIN2 primary antibody (1:1000) and Cyanine Dye3 (Cy3)-conjugated anti-rabbit secondary antibody (1:600) (Sigma) following a whole-mount procedure as described for *Arabidopsis* (Sauer et al., 2006). Images were acquired using a Zeiss LSM 700 upright confocal microscope. To quantify PIN2 distribution in root epidermal cells of wild type and *dgt*, measurements were performed with ImageJ2x software and analyzed with GraphPad Prism6 software. Obtained data were tested by Mann–Whitney test to assess significance. The PIN2 levels inside the cell were measured as the mean gray value of pixel intensity using the 'poligon' option, and the PIN2 levels at the plasma membrane as the mean gray value of pixel intensity using the 'segmented lines' option with 'line width' set to three pixels. For each cell, the distribution of the PIN2 signal across the membrane was measured in pixels as the length of the area possessing PIN2 signal ('thickness' of the PM signal). The distribution of the PIN2 signal along the same plasma membrane (length of the PM domain with signal) was measured to normalize for differences in cell size.

Acknowledgements

We thank S. Napsucialy-Mendivil, L. Charrier (Department of Biology, University of Fribourg, Switzerland) and Kathy Cook (Microtechniques Laboratory, Oregon State University, USA) for technical assistance; Hideriro Fukaki (Department of Biology, Kobe University, Japan) for the *IAA14:mIAA14-GFP* construct; Chris Kuhlemeyer (Institute of Plant Sciences, University of Bern, Switzerland) for the tomato PIN1a sequence; Charles Gasser (University of California Davis, USA) for cyclophilin A antibody; M. J. Ek Ramos and T. P. Devarenne (Department of Biochemistry and Biophysics, Texas A&M University, USA) for advice in tomato protoplast preparation; and The Tomato Genetics Resource Center at University of California, Davis (http://tgrc.ucdavis.edu/) for seeds of the *entire* (*e*) and *Epinastic* (*Epi*) tomato mutants.

Competing interests

The authors declare no competing or financial interests.

Author contributions

M.G.I., M.G. and J.F. designed experiments. M.G.I. generated expression constructs, prepared transgenic *Arabidopsis* and tomato lines, analyzed reporter expression, generated and analyzed *dgt e* mutants, and performed grafting experiments. J.Z. and B.W. performed PAT measurements in tomato, *N. benthamiana* and *S. cerevisiae* auxin transport assays, and confocal microscope imaging of protein localization. E.M. analyzed PIN1 and PIN2 expression in tomato root tips. Y.D. analyzed PIN expression in response to BFA treatment. E.A. and S.M. performed measurements of IAA fluxes with an IAA-specific microelectrode. M.M. performed statistical analysis of PIN expression in BFA-treated roots. S.F. performed RT-qPCR of *PIN* mRNA expression. J.G.D. performed confocal microscope analyses of *DGT:mCherry* expression in *Arabidopsis* roots. M.G.I. wrote the paper with inputs from M.G. and J.F. All authors participated with data analysis and interpretation.

Funding

Financial support was provided by the USDA National Research Initiative Competitive Grants Program [2007-35304-17728 to M.G.I.], by the Oregon State University General Research Fund (to M.G.I.), by PRIN 2010-11 'PRO-ROOT' (to S.M.), by Mexican CONACyT [127957, J.G.D.], by PAPIIT-DGAPA, by Universidad Nacional Autónoma de México [IN204312 to J.G.D.], by the Odysseus program of Research Foundation-Flanders (J.F.), by the Pool de Recherche of the University of Fribourg (M.G.), by the Novartis Foundation (M.G.) and by Swiss National Funds (M.G.).

Supplementary material

Supplementary material available online.

References

Ansari, H., Greco, G. and Luban, J. (2002). Cyclophilin A peptidyl-prolyl isomerase activity promotes ZPR1 nuclear export. *Mol. Cell. Biol.* **22**, 6993-7003.

Arévalo-Rodríguez, M. and Heitman, J. (2005). Cyclophilin A is localized to the nucleus and controls meiosis in Saccharomyces cerevisiae. *Eukaryot. Cell* **4**, 17-29.

Arévalo-Rodríguez, M., Cardenas, M. E., Wu, X., Hanes, S. D. and Heitman, J. (2000). Cyclophilin A and Ess1 interact with and regulate silencing by the Sin3-Rpd3 histone deacetylase. *EMBO J.* **19**, 3739-3749.

Balbi, V. and Lomax, T. L. (2003). Regulation of early tomato fruit development by the diageotropica gene. *Plant Phys.* **131**, 186-197.

Bayer, E. M., Smith, R. S., Mandel, T., Nakayama, N., Sauer, M., Prusinkiewicz, P. and Kuhlemeier, C. (2009). Integration of transport-based models for phyllotaxis and midvein formation. *Genes Dev.* **23**, 373-384.

Benková, E., Michniewicz, M., Sauer, M., Teichmann, T., Seifertová, D., Jürgens, G. and Friml, J. (2003). Local, efflux-dependent auxin gradients as a common module for plant organ formation. *Cell* **115**, 591-602.

Benková, E., Ivanchenko, M. G., Friml, J., Shishkova, S. and Dubrovsky, J. G. (2009). A morphogenetic trigger: is there an emerging concept in plant developmental biology? *Trends Plant Sci.* **14**, 189-193.

Bhalerao, R. P., Eklöf, J., Ljung, K., Marchant, A., Bennett, M. and Sandberg, G. (2002). Shoot-derived auxin is essential for early lateral root emergence in Arabidopsis seedlings. *Plant J.* **29**, 325-332.

Bishopp, A., Lehesranta, S., Vatén, A., Help, H., El-Showk, S., Scheres, B., Helariutta, K., Mähönen, A. P., Sakakibara, H. and Helariutta, Y. (2011). Phloem-transported cytokinin regulates polar auxin transport and maintains vascular pattern in the root meristem. *Curr. Biol.* **21**, 927-932.

Blakeslee, J. J., Bandyopadhyay, A., Lee, O. R., Mravec, J., Titapiwatanakun, B., Sauer, M., Makam, S. N., Cheng, Y., Bouchard, R., Adamec, J. et al. (2007). Interactions among PIN-FORMED and P-glycoprotein auxin transporters in Arabidopsis. *Plant Cell* **19**, 131-147.

Blilou, I., Xu, J., Wildwater, M., Willemsen, V., Paponov, I., Friml, J., Heidstra, R., Aida, M., Palme, K. and Scheres, B. (2005). The PIN auxin efflux facilitator network controls growth and patterning in Arabidopsis roots. *Nature* **433**, 39-44.

Bouchard, R., Bailly, A., Blakeslee, J. J., Oehring, S. C., Vincenzetti, V., Lee, O. R., Paponov, I., Palme, K., Mancuso, S., Murphy, A. S. et al. (2006). Immunophilin-like TWISTED DWARF1 modulates auxin efflux activities of Arabidopsis P-glycoproteins. *J. Biol. Chem.* **281**, 30603-30612.

Brazin, K. N., Mallis, R. J., Fulton, D. B. and Andreotti, A. H. (2002). Regulation of the tyrosine kinase Itk by the peptidyl-prolyl isomerase cyclophilin A. *Proc. Natl. Acad. Sci. USA* **99**, 1899-1904.

Casimiro, I., Marchant, A., Bhalerao, R. P., Beeckman, T., Dhooge, S., Swarup, R., Graham, N., Inzé, D., Sandberg, G., Casero, P. J. et al. (2001). Auxin transport promotes Arabidopsis lateral root initiation. *Plant Cell* **13**, 843-852.

Christian, M., Steffens, B., Schenck, D. and Lüthen, H. (2003). The diageotropica mutation of tomato disrupts a signalling chain using extracellular auxin binding protein 1 as a receptor. *Planta* **218**, 309-314.

Colgan, J., Asmal, M., Neagu, M., Yu, B., Schneidkraut, J., Lee, Y., Sokolskaja, E., Andreotti, A. and Luban, J. (2004). Cyclophilin A regulates TCR signal strength in CD4+ T cells via a proline-directed conformational switch in Itk. *Immunity* **21**, 189-201.

Daniel, S. G., Rayle, D. L. and Cleland, R. E. (1989). Auxin physiology of the tomato mutant diageotropica. *Plant Physiol.* **91**, 804-807.

De Smet, I., Tetsumura, T., De Rybel, B., Frey, N. F. d., Laplaze, L., Casimiro, I., Swarup, R., Naudts, M., Vanneste, S., Audenaert, D. et al. (2007). Auxin-

dependent regulation of lateral root positioning in the basal meristem of Arabidopsis. *Development* **134**, 681-690.

Dubrovsky, J. G., Sauer, M., Napsucialy-Mendivil, S., Ivanchenko, M. G., Friml, J., Shishkova, S., Celenza, J. and Benková, E. (2008). Auxin acts as a local morphogenetic trigger to specify lateral root founder cells. *Proc. Natl. Acad. Sci. USA* **105**, 8790-8794.

Dubrovsky, J. G., Napsucialy-Mendivil, S., Duclercq, J., Cheng, Y., Shishkova, S., Ivanchenko, M. G., Friml, J., Murphy, A. S. and Benková, E. (2011). Auxin minimum defines a developmental window for lateral root initiation. *New Phytol.* **191**, 970-983.

Fujino, D. W., Burger, D. W., Yang, S. F. and Bradford, K. J. (1988). Characterization of an ethylene overproducing mutant of tomato (Lycopersicon esculentum Mill. Cultivar VFN8). *Plant Physiol.* **88**, 774-779.

Fukaki, H., Tameda, S., Masuda, H. and Tasaka, M. (2002). Lateral root formation is blocked by a gain-of-function mutation in the SOLITARY-ROOT/IAA14 gene of Arabidopsis. *Plant J.* **29**, 153-168.

Galigniana, M. D., Morishima, Y., Gallay, P. A. and Pratt, W. B. (2004). Cyclophilin-A is bound through its peptidylprolyl isomerase domain to the cytoplasmic dynein motor protein complex. *J. Biol. Chem.* **279**, 55754-55759.

Geldner, N., Friml, J., Stierhof, Y.-D., Jürgens, G. and Palme, K. (2001). Auxin transport inhibitors block PIN1 cycling and vesicle trafficking. *Nature* **413**, 425-428.

Grunewald, W. and Friml, J. (2010). The march of the PINs: developmental plasticity by dynamic polar targeting in plant cells. *EMBO J.* **29**, 2700-2714.

Henrichs, S., Wang, B., Fukao, Y., Zhu, J., Charrier, L., Bailly, A., Oehring, S. C., Linnert, M., Weiwad, M., Endler, A. et al. (2012). Regulation of ABCB1/PGP1-catalysed auxin transport by linker phosphorylation. *EMBO J.* **31**, 2965-2980.

Himanen, K., Boucheron, E., Vanneste, S., de Almeida Engler, J., Inzé, D. and Beeckman, T. (2002). Auxin-mediated cell cycle activation during early lateral root initiation. *Plant Cell* **14**, 2339-2351.

Ivanchenko, M. G., Coffeen, W. C., Lomax, T. L. and Dubrovsky, J. G. (2006). Mutations in the Diageotropica (Dgt) gene uncouple patterned cell division during lateral root initiation from proliferative cell division in the pericycle. *Plant J.* **46**, 436-447.

Ivanchenko, M. G., den Os, D., Monshausen, G. B., Dubrovsky, J. G., Bednárová, A. and Krishnan, N. (2013). Auxin increases the hydrogen peroxide (H_2O_2) concentration in tomato (Solanum lycopersicum) root tips while inhibiting root growth. *Ann. Bot.* **112**, 1107-1116.

Kang, B., Zhang, Z., Wang, L., Zheng, L., Mao, W., Li, M., Wu, Y., Wu, P. and Mo, X. (2013). OsCYP2, a chaperone involved in degradation of auxin-responsive proteins, plays crucial roles in rice lateral root initiation. *Plant J.* **74**, 86-97.

Kim, J.-Y., Henrichs, S., Bailly, A., Vincenzetti, V., Sovero, V., Mancuso, S., Pollmann, S., Kim, D., Geisler, M. and Nam, H.-G. (2010). Identification of an ABCB/P-glycoprotein-specific inhibitor of auxin transport by chemical genomics. *J. Biol. Chem.* **285**, 23309-23317.

Kleine-Vehn, J., Dhonukshe, P., Sauer, M., Brewer, P. B., Wiśniewska, J., Paciorek, T., Benková, E. and Friml, J. (2008). ARF GEF-dependent transcytosis and polar delivery of PIN auxin carriers in Arabidopsis. *Curr. Biol.* **18**, 526-531.

Lavenus, J., Lucas, M., Laplaze, L. and Guyomarc'h, S. (2013a). The dicot root as a model system for studying organogenesis. *Methods Mol. Biol.* **959**, 45-67.

Lavenus, J., Goh, T., Roberts, I., Guyomarc'h, S., Lucas, M., De Smet, I., Fukaki, H., Beeckman, T., Bennett, M. and Laplaze, L. (2013b). Lateral root development in Arabidopsis: fifty shades of auxin. *Trends Plant Sci.* **18**, 450-458.

Lavy, M., Prigge, M. J., Tigyi, K. and Estelle, M. (2012). The cyclophilin DIAGEOTROPICA has a conserved role in auxin signaling. *Development* **139**, 1115-1124.

Lewis, D. R. and Muday, G. K. (2009). Measurement of auxin transport in Arabidopsis thaliana. *Nat. Protoc.* **4**, 437-451.

Lippuner, V., Chou, I. T., Scott, S. V., Ettinger, W. F., Theg, S. M. and Gasser, C. S. (1994). Cloning and characterization of chloroplast and cytosolic forms of cyclophilin from Arabidopsis thaliana. *J. Biol. Chem.* **269**, 7863-7868.

Lu, Y.-C., Song, J., Cho, H.-Y., Fan, G., Yokoyama, K. K. and Chiu, R. (2006). Cyclophilin A protects Peg3 from hypermethylation and inactive histone modification. *J. Biol. Chem.* **281**, 39081-39087.

Malamy, J. E. and Benfey, P. N. (1997). Organization and cell differentiation in lateral roots of Arabidopsis thaliana. *Development* **124**, 33-44.

Mancuso, S., Marras, A. M., Magnus, V. and Baluška, F. (2005). Noninvasive and continuous recordings of auxin fluxes in intact root apex with a carbon nanotube-modified and self-referencing microelectrode. *Anal. Biochem.* **341**, 344-351.

Marchant, A., Kargul, J., May, S. T., Muller, P., Delbarre, A., Perrot-Rechenmann, C. and Bennett, M. J. (1999). AUX1 regulates root gravitropism in Arabidopsis by facilitating auxin uptake within root apical tissues. *EMBO J.* **18**, 2066-2073.

Mignolli, F., Mariotti, L., Lombardi, L., Vidoz, M. L., Ceccarelli, N. and Picciarelli, P. (2012). Tomato fruit development in the auxin-resistant dgt mutant is induced by pollination but not by auxin treatment. *J. Plant Physiol.* **169**, 1165-1172.

Mito, N. and Bennett, A. B. (1995). The diageotropica mutation and synthetic auxins differentially affect the expression of auxin-regulated genes in tomato. *Plant Physiol.* **109**, 293-297.

Moreno-Risueno, M. A., Van Norman, J. M., Moreno, A., Zhang, J., Ahnert, S. E. and Benfey, P. N. (2010). Oscillating gene expression determines competence for periodic Arabidopsis root branching. *Science* **329**, 1306-1311.

Mravec, J., Skůpa, P., Bailly, A., Hoyerová, K., Křeček, P., Bielach, A., Petrášek, J., Zhang, J., Gaykova, V., Stierhof, Y.-D. et al. (2009). Subcellular homeostasis of phytohormone auxin is mediated by the ER-localized PIN5 transporter. *Nature* **459**, 1136-1140.

Muday, G. K., Lomax, T. L. and Rayle, D. L. (1995). Characterization of the growth and auxin physiology of roots of the tomato mutant, diageotropica. *Planta* **195**, 548-553.

Nebenführ, A., White, T. J. and Lomax, T. L. (2000). The diageotropica mutation alters auxin induction of a subset of the Aux/IAA gene family in tomato. *Plant Mol. Biol.* **44**, 73-84.

Oh, K., Ivanchenko, M. G., White, T. J. and Lomax, T. L. (2006). The diageotropica gene of tomato encodes a cyclophilin: a novel player in auxin signaling. *Planta* **224**, 133-144.

Overvoorde, P., Fukaki, H. and Beeckman, T. (2010). Auxin control of root development. *Cold Spring Harb. Perspect. Biol.* **2**, pa001537.

Paciorek, T., Zazímalová, E., Ruthardt, N., Petrášek, J., Stierhof, Y.-D., Kleine-Vehn, J., Morris, D. A., Emans, N., Jürgens, G., Geldner, N. et al. (2005). Auxin inhibits endocytosis and promotes its own efflux from cells. *Nature* **435**, 1251-1256.

Pijnappel, W. W. M. P., Schaft, D., Roguev, A., Shevchenko, A., Tekotte, H., Wilm, M., Rigaut, G., Séraphin, B., Aasland, R. and Stewart, A. F. (2001). The S. cerevisiae SET3 complex includes two histone deacetylases, Hos2 and Hst1, and is a meiotic-specific repressor of the sporulation gene program. *Genes Dev.* **15**, 2991-3004.

Reed, R. C., Brady, S. R. and Muday, G. K. (1998). Inhibition of auxin movement from the shoot into the root inhibits lateral root development in Arabidopsis. *Plant Physiol.* **118**, 1369-1378.

Robert, S., Kleine-Vehn, J., Barbez, E., Sauer, M., Paciorek, T., Baster, P., Vanneste, S., Zhang, J., Simon, S., Čovanová, M. et al. (2010). ABP1 mediates auxin inhibition of clathrin-dependent endocytosis in Arabidopsis. *Cell* **143**, 111-121.

Santelia, D., Vincenzetti, V., Azzarello, E., Bovet, L., Fukao, Y., Düchtig, P., Mancuso, S., Martinoia, E. and Geisler, M. (2005). MDR-like ABC transporter AtPGP4 is involved in auxin-mediated lateral root and root hair development. *FEBS Lett.* **579**, 5399-5406.

Sauer, M., Paciorek, T., Benková, E. and Friml, J. (2006). Immunocytochemical techniques for whole-mount in situ protein localization in plants. *Nat. Protocols* **1**, 98-103.

Schiene-Fischer, C. and Yu, C. (2001). Receptor accessory folding helper enzymes: the functional role of peptidyl prolyl cis/trans isomerases. *FEBS Lett.* **495**, 1-6.

Sorin, M. and Kalpana, G. V. (2006). Dynamics of virus-host interplay in HIV-1 replication. *Curr. HIV Res.* **4**, 117-130.

Turnbull, C. G. N., Booker, J. P. and Leyser, H. M. O. (2002). Micrografting techniques for testing long-distance signalling in Arabidopsis. *Plant J.* **32**, 255-262.

Vanneste, S. and Friml, J. (2009). Auxin: a trigger for change in plant development. *Cell* **136**, 1005-1016.

Vieten, A., Vanneste, S., Wiśniewska, J., Benková, E., Benjamins, R., Beeckman, T., Luschnig, C. and Friml, J. (2005). Functional redundancy of PIN proteins is accompanied by auxin-dependent cross-regulation of PIN expression. *Development* **132**, 4521-4531.

Wan, Y., Jasik, J., Wang, L., Hao, H., Volkmann, D., Menzel, D., Mancuso, S., Baluška, F. and Lin, J. (2012). The signal transducer NPH3 integrates the phototropin1 photosensor with PIN2-based polar auxin transport in Arabidopsis root phototropism. *Plant Cell* **24**, 551-565.

Wang, P. and Heitman, J. (2005). The cyclophilins. *Genome Biol.* **6**, 226.

Wang, H., Jones, B., Li, Z., Frasse, P., Delalande, C., Regad, F., Chaabouni, S., Latché, A., Pech, J.-C. and Bouzayen, M. (2005). The tomato Aux/IAA transcription factor IAA9 is involved in fruit development and leaf morphogenesis. *Plant Cell* **17**, 2676-2692.

Wang, B., Bailly, A., Zwiewka, M., Henrichs, S., Azzarello, E., Mancuso, S., Maeshima, M., Friml, J., Schulz, A. and Geisler, M. (2013). Arabidopsis TWISTED DWARF1 functionally interacts with auxin exporter ABCB1 on the root plasma membrane. *Plant Cell* **25**, 202-214.

Wu, G., Otegui, M. S. and Spalding, E. P. (2010). The ER-localized TWD1 immunophilin is necessary for localization of multidrug resistance-like proteins required for polar auxin transport in Arabidopsis roots. *Plant Cell* **22**, 3295-3304.

Wu, J., Peng, Z., Liu, S., He, Y., Cheng, L., Kong, F., Wang, J. and Lu, G. (2012). Genome-wide analysis of Aux/IAA gene family in Solanaceae species using tomato as a model. *Mol. Genet. Genomics* **287**, 295-311.

Zander, K., Sherman, M. P., Tessmer, U., Bruns, K., Wray, V., Prechtel, A. T., Schubert, E., Henklein, P., Luban, J., Neidleman, J. et al. (2003). Cyclophilin A interacts with HIV-1 Vpr and is required for its functional expression. *J. Biol. Chem.* **278**, 43202-43213.

Zhang, J., Chen, R., Xiao, J., Qian, C., Wang, T., Li, H., Ouyang, B. and Ye, Z. (2007). A single-base deletion mutation in SlIAA9 gene causes tomato (Solanum lycopersicum) entire mutant. *J. Plant Res.* **120**, 671-678.

Zheng, H., Li, S., Ren, B., Zhang, J., Ichii, M., Taketa, S., Tao, Y., Zuo, J. and Wang, H. (2013). LATERAL ROOTLESS2, a cyclophilin protein, regulates lateral root initiation and auxin signaling pathway in rice. *Mol. Plant.* **6**, 1719-1721.

Zobel, R. W. (1973). Control of morphogenesis in the ethylene-requiring tomato mutant, diageotropica. *Can. J. Bot.* **52**, 735-741.